scientific reports

Check for updates

OPEN

# Methylcobalamin-containing nanofiber sheets have better neuroprotective effects than small intestinal submucosa sheets

Yoshiaki Yoshimura[1], Toru Iwahashi[1], Taisuke Kasuya[1], Toshiki Shimada[1], Katsuyuki Konishi[1], Atsushi Kamata[1], Mai Konishi[1], Arisa Kazui[2], Ryoya Shiode[2], Satoshi Miyamura[2], Kunihiro Oka[2], Seiji Okada[1] & Hiroyuki Tanaka[3]✉

**Postoperative adhesion around nerves sometimes results in sensory and motor dysfunctions. To prevent these disorders, we have developed an electrospun nanofiber sheet incorporating methylcobalamin (MeCbl), an active form of vitamin B12 with anti-inflammatory and neuroregenerative effects. This study aimed to investigate the neuroprotective effects of MeCbl sheets against postoperative adhesion and to compare the effects of MeCbl sheets with those of porcine small intestinal submucosa (SIS) sheets using a rat sciatic nerve adhesion model. Behavioral and electrophysiological analyses showed superior results in the MeCbl sheet group compared with those in the untreated group, all of which were non-inferior to the SIS sheet group. Histological analysis revealed less collagen and inflammatory cell invasion into the nerve parenchyma and a higher number of residual axons and myelination rate in the MeCbl sheet group than in the untreated group. Moreover, the MeCbl sheet group was superior to the SIS sheet group in terms of the myelination rate and decreased number of infiltrating macrophages. Furthermore, the distribution of residual axons by diameter revealed that the MeCbl sheet group had thicker axons than the SIS sheet group. The use of MeCbl sheets may represent a novel approach for preventing secondary nervous system impairment following inflammation.**

In the treatment of constrictive neuropathies, such as carpal tunnel syndrome and cubital tunnel syndrome, nerve decompression and neurolysis are generally performed with favorable outcomes[1–4]. However, postoperative inflammation and scarring lead to adhesions between nerves and surrounding tissues, which impair the physiological glide of the nerves, inhibit axonal extension due to the infiltration of scar tissues into the nerve, and cause demyelination, impaired blood flow, and axonal degeneration due to compression, resulting in associated sensory and motor dysfunctions[5–8]. Once inflammation occurs in the soft tissues around the nerves, scar tissue formation occurs both inside and outside the nerves, resulting in adhesions[5–8]. In general, local inflammation promotes vascular hyperpermeability; migration of leukocytes, including macrophages; and fibrin deposition at the site of inflammation. Macrophages produce several types of growth factors, such as transforming growth factor-beta, insulin-like growth factor, macrophage-derived growth factor, and fibroblast growth factor, attracting endothelial cells and fibroblasts to the site of injury[9–12], followed by the deposition of collagen fibers and the formation of scars and granulation tissues, leading to adhesions of soft tissues. These inflammatory reactions persist for approximately 1–3 weeks postoperatively[13], during which protecting nerves from inflammatory infiltration and scar tissues is crucial for preventing adhesions and subsequent nerve damage. To minimize postoperative inflammation and prevent subsequent nerve adhesions, surgical loupes and microscopes are used to reduce surgical damage caused by patronizing manipulations on the tissue, and soft tissue flaps, such as veins and fat valves, are used to cover the nerve[3,4,14–16]. However, for cases with severe tissue damage, such as in severe trauma, reduction of surgical damage alone is insufficient. Additionally, soft tissue covering is not a generalized method because of the complexity of the procedure and the possibility of inducing other disorders, such as donor site morbidity and sensory disturbance. For these reasons, several nerve-protective materials and

[1]Department of Orthopaedic Surgery, Osaka University Graduate School of Medicine, 2-2 Yamadaoka, Suita, Osaka 565-0871, Japan. [2]Department of Orthopaedic Biomaterial Science, Osaka University Graduate School of Medicine, 2-2 amadaoka, Suita, Osaka 565-0871, Japan. [3]Department of Sports Medical Science, Osaka University Graduate School of Medicine, 2-2 Yamadaoka, Suita, Osaka 565-0871, Japan. ✉email: tanaka.hiroyuki.med@osaka-u.ac.jp

methods have been developed in recent years, and their efficacies have been reported[17–26]. Historically, there have been reports on the protection of peripheral nerves using techniques, such as vein wrapping or placing muscle or fat flaps[14–16,27,28]. Nonetheless, the possibility of complications, such as scarring at the donor site, has led to the development of alternative materials of nerve protection, including silicone sheets, biodegradable sheets composed of poly(L-lactide) and poly(e-caprolactone) (PCL), collagen gels, and sheets[17,18,21–26]. However, symptom recurrence cannot be sufficiently prevented[7]and no ideal treatment for peripheral nerve scarring exists in clinical settings. To prevent these unfavorable events, it is important to protect nerves from postoperative inflammation and scar formation[7,20,24,26,29]. Therefore, new treatment methods are being developed. Several reports have described neuroprotective materials that are implanted around the nerve to act as a physical barrier to maintain physiological stretching and sliding of the nerve and to inhibit fibrosis and cellular infiltration inside and outside the nerve[17–22,30]. Recently, artificial nerves used for nerve defects have been reported to be effective against nerve adhesions. Shintani et al. reported that a tube composed of polylactic acid and PCL suppressed adhesions and significantly reduced nerve damage [29]. However, materials that prevent adhesions by acting on the inflammatory healing process have also been studied, with reports that perineural scar formation was reduced by covering the nerve with membrane tissues that release methylprednisolone, which inhibits fibroblasts and granulocytes[31], and that intraperitoneal administration of minocycline, used as an antibacterial agent, inhibited polarity changes to inflammatory macrophages, reducing perineural scar formation and nerve damage[32]. Although some of these implants have been used in clinical practice with generally positive results[24,31], the results have not been consistent. Additionally, a gold standard for treatment has not yet been established in terms of the risks of side effects of the released drug and the manufacturing cost of implants. Therefore, there is an urgent need to develop standardized implants that can be used in clinical practice.

To address these issues, we focused specifically on methylcobalamin (MeCbl). MeCbl, an active form of vitamin B12, is used worldwide for the treatment of peripheral neuropathy owing to its low cost and minimal side effects and has great potential for regulating inflammation and promoting nerve regeneration[33]. In our previous study, we revealed that high concentrations of MeCbl activated ERK and AKT in dorsal root ganglion neurons through the methylation cycle, promoting the survival of nerve cells and regeneration of peripheral nerves in vivo and improving motor and sensory functions after peripheral nerve injury in vivo[34–36]. Moreover, vitamin B12 exerts an anti-inflammatory effect by accelerating macrophage polarization from proinflammatory (M1) to an anti-inflammatory (M2) phenotype[37]. Additionally, Suzuki et al. reported that axonal outgrowth was promoted even when MeCbl was applied only to the axons of rat cortical neurons, suggesting that the local administration of MeCbl to peripheral nerves is effective[38]. However, when a high-concentration dose is administered in clinical use, there are some problems, such as the short half-life of MeCbl, which requires frequent injections to maintain therapeutic blood concentrations, and the route of administration[39]. To compensate for these problems, we have engineered a biodegradable nerve-protective nanofiber sheet containing MeCbl, termed the MeCbl sheet, allowing local sustained release and achievement of an effective high concentration of MeCbl. In our previous study, we reported that the MeCbl sheet released MeCbl in an in vitro environment for up to 38 weeks after implantation and that the local concentration of MeCbl was significantly higher in the implantation group than in the non-implantation group in an in vivo rat model[38]. Using rat sciatic nerve crush injury, sciatic nerve transection, and defect models, we reported the efficacy of MeCbl sheets for the promotion of peripheral nerve regeneration[38,40,41]. However, the neuroprotective effect of MeCbl sheets against post-inflammatory scarring and adhesions around the peripheral nerve and their superiority over competing products remain unclear. Hence, this study aimed to evaluate the neuroprotective effects of the MeCbl sheets against postsurgical adhesions and to compare the effects of the MeCbl sheets with those of porcine small intestinal submucosa (SIS) sheets, which are useful neuroprotective implant to prevent perineural adhesions and used in clinical practice[20,24,30]. We hypothesized that MeCbl sheet, a synthetic nanofiber wrap containing MeCbl, would have superior anti-inflammatory effects and subsequent neuroregenerative effects over SIS sheet, a material derived from a different species that can cause peri-implant inflammation.

## Methods

### Preparation of methylcobalamin sheets

We prepared MeCbl sheets (Fig. 1a) in the same manner as previously reported[19]. Briefly, the MeCbl sheets were created by electrospinning a mixture of PCL and MeCbl at an applied voltage of 20 kV (Nanon-01 A; MECC Co., Ltd., Fukuoka, Japan) with collector plate separation and a 24-gauge needle. The flow rate was 1.0 mL/h. The PCL/solvent ratio (w/v) was 10wt%. The weight ratio of MeCbl to PCL in the MeCbl sheets was 3%.

### Animals

All experiments were approved (approval number J007998-004) by the Ethics Review Committee for Animal Experimentation at Osaka University. Thirty 6-week-old male Wistar rats (weight, 180–220 g; Charles River Laboratories, Tokyo, Japan) were used in this study. The rats were monitored daily in a temperature-controlled central animal facility with free access to chow and water. This study was conducted in accordance with the ARRIVE guidelines, and all methods described below were performed in accordance with the relevant guidelines and regulations.

### Surgical procedures

The rats were anesthetized with a subcutaneously injected mixture of midazolam (2 mg/kg), butorphanol (2.5 mg/kg), and medetomidine (0.15 mg/kg). The left sciatic nerve was exposed to sterile conditions and released from the surrounding tissues in the area spanning from the sciatic notch to its trifurcation. To stimulate the local fibrotic responses, the surface of the neural bed was repeatedly burned using a bipolar coagulator (Bovie Medical Corporation, Clearwater, FL). Subsequently, the epineurium and perineurium were carefully

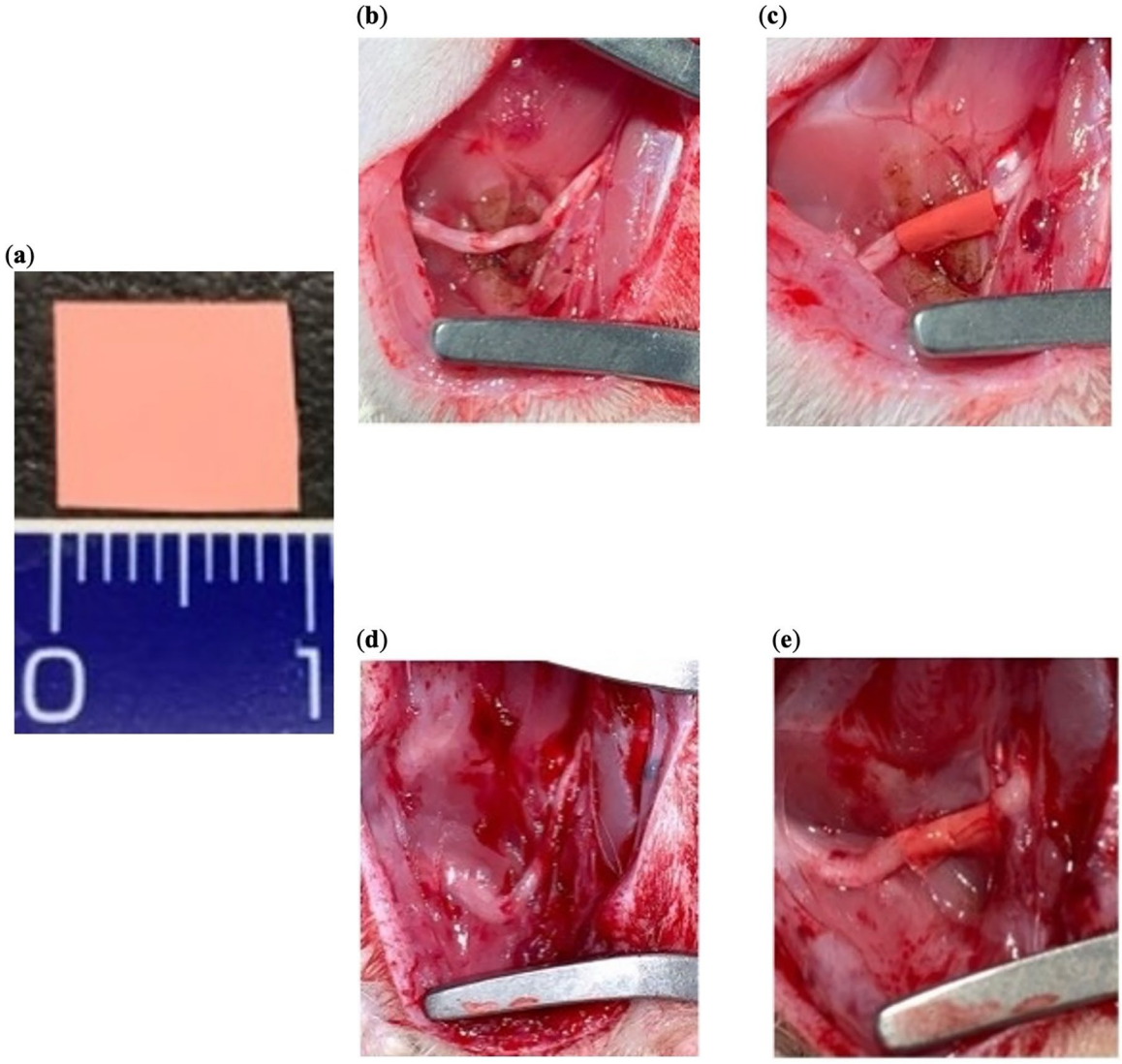


**Fig. 1**. Methylcobalamin (MeCbl) sheet and intraoperative gross findings of rat sciatic nerve. (**a**) For implantation, MeCbl sheet was cut to a size of 10 × 7 mm. (**b**) Untreated group, in which the soft tissue around the sciatic nerve was burned using a bipolar coagulator, followed by stripping, without any subsequent treatment. (**c**) MeCbl sheet group, in which the soft tissue around the sciatic nerve was burned using a bipolar coagulator followed by stripping and wrapping of the sciatic nerve with an MeCbl sheet. (**d**) Untreated group 2 weeks postoperatively. (**e**) MeCbl sheet group 2 weeks postoperatively.

removed circumferentially and stripped distally by 8 mm, with careful attention to avoid damage to the axons (Fig. 1b). The rats were randomized to four groups: sham group ($n = 4$), in which only the sciatic nerve was exposed without the epi- and perineurectomy or burning the surface of the neural bed; untreated group ($n = 10$), in which no treatment after the injury was performed; MeCbl sheet group ($n = 8$), in which the sciatic nerve was wrapped in an MeCbl sheet after the injury (10 × 7 mm) (Fig. 1c); and SIS sheet group ($n = 8$), in which the sciatic nerve was wrapped in a SIS sheet after the injury (10 × 7 mm). The fascia and skin were closed using 4 − 0 nylon sutures. The same surgeon performed all procedures and was blinded to the animals assigned to each group. Two weeks after surgery, the rats were euthanized with an overdose of sodium pentobarbital, and the left sciatic nerve was harvested from each implant (Fig. 1d, e).

## von Frey filament test

The von Frey filament test was performed to assess the mechanical sensitivity 2 weeks postoperatively. The paw withdrawal threshold was measured, as previously described (0.008–300 g; TouchTest; North Coast Medical, Morgan Hill, CA, USA)[42,43]. Briefly, the rats were placed on a metal mesh plate, and from a point 1.5 cm away from the hind limb, the filament was brought into contact with the sole of the foot for 1 s and then gradually pressed for another 1 s. The weights of the filaments were recorded when proper withdrawal behavior was observed. The same procedure was performed on the contralateral hind limb, and the ipsilateral/contralateral ratio was calculated.

### Hargreaves test
The paw withdrawal threshold was measured to assess thermal sensitivity 2 weeks postoperatively. The Hargreaves test was performed as previously reported[44,45]. Briefly, the rats were placed on a glass chamber, and the paw planter surface was thermally stimulated using infrared irradiation equipment (I.R. Heat - Flux Radiometer; Ugo Basile, Varese, Italy) at 52.5 °C. The latency to paw withdrawal behavior was measured, and the ipsilateral/contralateral ratio was calculated.

### Isometric tetanic force test
To assess motor function, an isometric tetanic force analysis was performed 2 weeks postoperatively, as previously described[46]. The tibialis anterior muscle was meticulously separated from the tibia, and the muscle tendon was detached and subsequently affixed to a force transducer. To immobilize the hind limbs, an 18G needle was inserted into the distal aspect of the femoral condyle and ankle joint, securing them onto a cork board. Bipolar stimulating electrodes were placed on the sciatic nerve at the level of the sciatic notch, and the stimulus was applied. The force transducer signal was processed using a PowerLab device and software (PowerLab; AD Instruments, Bella Vista, Australia). The maximum isometric tetanic force was determined as the highest force plateau.

### Wet muscle weight of the tibialis anterior
Wet muscle weight was measured to evaluate motor function. The tibialis anterior muscle on the experimental side 2 weeks postoperatively was harvested and weighed.

### Electrophysiology
Electrophysiological analyses were performed 2 weeks postoperatively. Bipolar stimulating electrodes were placed on the sciatic nerve at the level of the sciatic notch. Terminal latency (TL) and compound muscle action potential (CMAP) were recorded using electrodes inserted into the tibialis anterior muscle. Bipolar stimulating electrodes were also placed 10 mm distal to the level of proximal stimulation to calculate nerve conduction velocity (NCV). A PowerLab device and software (PowerLab; AD Instruments, Bella Vista, Australia) were used to detect and measure CMAP, TL, and NCV.

### Histology
Histomorphological analyses of the sciatic nerves at the midpoint of the operated site were performed 2 weeks postoperatively. The left sciatic nerves with the surrounding tissues and implanted sheet were harvested, fixed in 4% paraformaldehyde overnight, and soaked in 0.01 M phosphate-buffered saline (PBS) with 30% sucrose for 2 days. Neural tissues were frozen in frozen-section media (FSC 22 Frozen Section Media; Leica Biosystems, San Diego, CA, USA) and cut into 10 µm cross-sections onto glass slides. Masson's trichrome staining was performed to quantify collagen deposition. For each nerve, the percentage of intraneural collagen (intraneural collagen area/neural area) was calculated using a light microscope (BZ-X800; Keyence, Osaka, Japan) and ImageJ software (version 1.54f). For immunohistological staining, sections were blocked with PBS containing 5% Blocking one (Blocking one; Nacalai Tesque, Kyoto, Japan) and 10% bovine serum albumin for 30 min. Samples were incubated at 4 °C overnight using primary antibodies to neurofilament 200 (NF200) (1:1,000; N4142; Sigma-Aldrich, St Louis, MO, USA) and CD68 (1:200; ab31630; Abcam, Boston, MA, USA) or myelin basic protein (MBP) (1:1,000; NE1018; Calbiochem, San Diego, CA, USA) and then incubated at 20–25 ℃ for 1 h using the following secondary antibodies: Alexa Fluor 488 goat anti-rabbit immunoglobulin G (IgG) and Alexa Fluor 568 goat anti-mouse IgG (1:1,000; Life Technologies, Carlsbad, CA, USA). Nuclei were stained with Permafluor mounting solution containing 4',6-diamidino-2-phenylindole (DAPI) (D532; DOJINDO, Kumamoto, Japan). For each nerve, the number of intraneural DAPI + or CD68 + cells, number of axons, distribution of axon diameters, and myelination ratio (MBP + axon number/total axon number) were calculated using the ImageJ software (version 1.54f).

### Statistical analyses
Statistical analyses were performed using one-way analysis of variance, followed by Tukey–Kramer's multiple comparison test. The analyses were performed using E-Z R software (version 1.55)[47]. Data are expressed as the mean and standard error of the mean (SEM). Significance was set at $p < 0.05$.

## Results
### Sensory and motor functional evaluation
To evaluate the neuroprotective effect of MeCbl sheets against postoperative adhesion, sensory and motor functions were assessed 2 weeks postoperatively. The untreated group ($1.9 \pm 0.55$) showed a significantly lower response to the mechanical stimulus than the sham group ($1.0 \pm 0.12$, $p < 0.01$). However, mechanical sensitivity remained both in the MeCbl ($1.1 \pm 0.37$) and SIS ($1.3 \pm 0.65$) sheet groups, showing no significant difference compared with that in the sham group. The MeCbl sheet group showed significantly preserved mechanical sensory function compared with the untreated group ($p < 0.01$) (Fig. 2a). Similarly, the thermal sensitivity was significantly lower in the untreated group ($1.3 \pm 0.22$) than in the sham group ($1.0 \pm 0.12$, $p < 0.05$). However, there were no significant differences among the MeCbl ($1.0 \pm 0.08$), SIS ($1.1 \pm 0.18$), and sham groups. The MeCbl sheet group showed significantly higher thermal sensory function than the untreated group ($p < 0.05$) (Fig. 2b). To evaluate motor function, the isometric tetanic force was measured 2 weeks postoperatively. The untreated ($8.5 \pm 7.9$ g), MeCbl sheet ($9.3 \pm 6.3$ g), and SIS sheet ($7.0 \pm 4.2$ g) groups had significantly lower isometric tetanic force than the sham group ($37.3 \pm 10.5$ g, $p < 0.001$). There were no significant differences among the untreated, MeCbl, and SIS sheet groups (Fig. 2c). The wet weight of the tibialis anterior muscle 2 weeks postoperatively

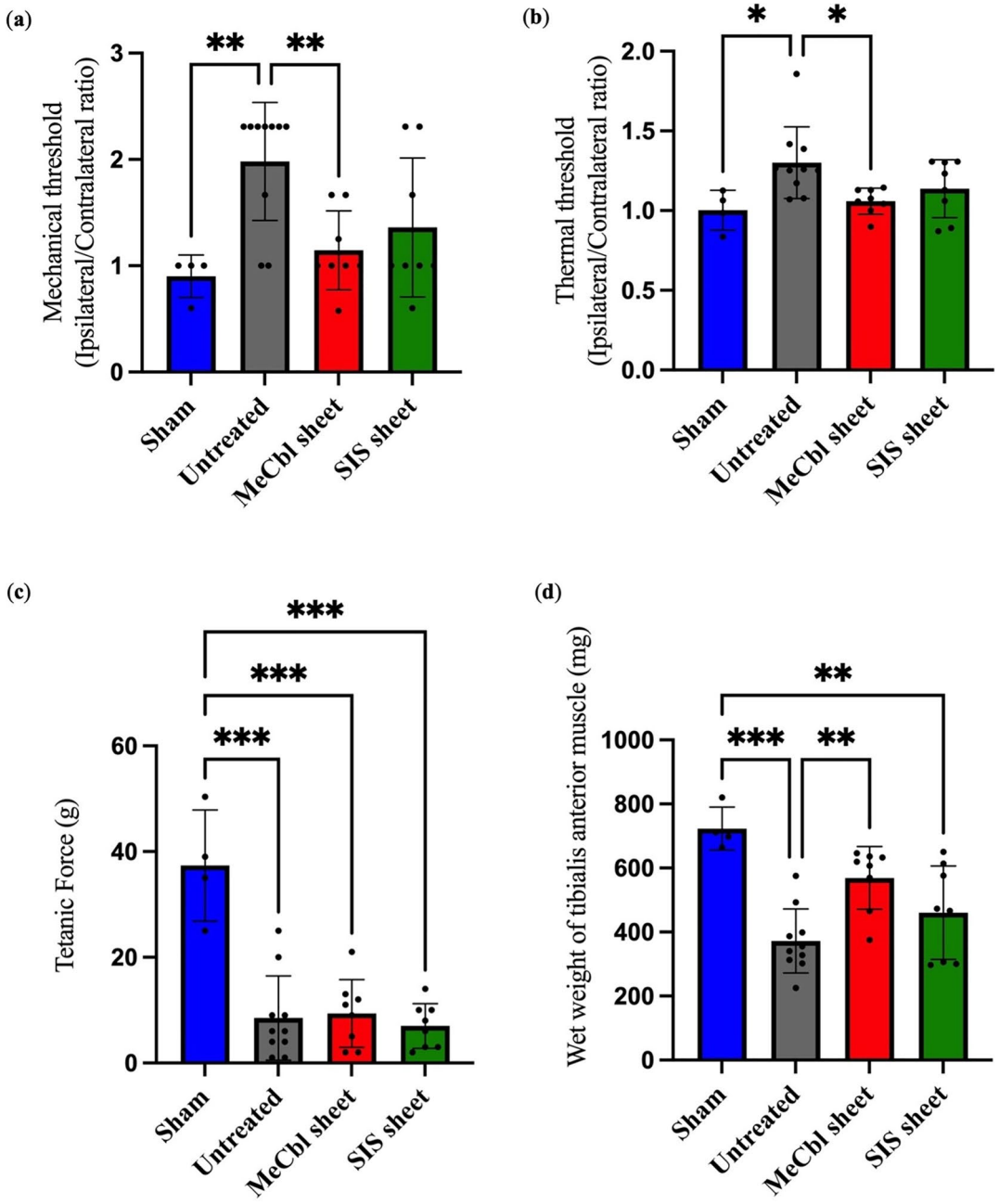


**Fig. 2**. Methylcobalamin (MeCbl) sheets mitigate the impairment in sensory function and decrease in tibialis anterior muscle wet weight. (**a**) von Frey filament test. (**b**) Hargreaves test. (**c**) Isometric tetanic force test. (**d**) Wet weight of the tibialis anterior muscle. $^{*}p < 0.05$, $^{**}p < 0.01$, and $^{***}p < 0.001$, one-way analysis of variance followed by Tukey–Kramer's test.

was significantly lower in the untreated ($371.7 \pm 100.0$ mg, $p < 0.001$) and SIS ($460.42 \pm 146.0$ mg, $p < 0.01$) sheet groups than in the sham group ($723.2 \pm 67.4$ mg). However, the MeCbl sheet group ($568.9 \pm 97.8$ mg) remained comparable to the sham group and had significantly higher wet weight of the tibialis anterior muscle than the untreated group ($p < 0.01$). There were no significant differences among the MeCbl and SIS sheets groups (Fig. 2d). These results indicate that MeCbl sheets are beneficial for maintaining sensory and motor functions after nerve adhesion injury.

## Electrophysiological evaluation

At 2 weeks postoperatively, CMAP amplitude was significantly lower in the untreated ($6.9 \pm 3.2$ mV, $p < 0.001$) and SIS ($12.7 \pm 7.8$ mV, $p < 0.01$) sheet groups than in the sham group ($29.4 \pm 9.3$ mV). However, there were no significant differences between the MeCbl ($18.2 \pm 10.0$ mV) and sham groups. The MeCbl sheet group showed significantly higher CMAP amplitude than the untreated group ($p < 0.05$) (Fig. 3a). NCV was also significantly

higher in the MeCbl sheet group (42.5 ± 8.3 mS) than in the untreated group (21.4 ± 8.1 mS, $p < 0.05$) (Fig. 3b). No significant differences were observed between the groups with respect to TL (Fig. 3c). These results suggest that MeCbl sheets may prevent nerve damage caused by inflammation and adhesions or hasten the recovery of peripheral nerves.

## Histological evaluation of the sciatic nerve

To examine the neuroprotective effects of MeCbl sheets in more detail, histological evaluation was performed. The amount of intraneural collagen deposition during scar formation was measured to investigate intraneural scarring 2 weeks after perineurectomy of the sciatic nerves using Masson's trichrome staining (Fig. 4a, b). Significantly higher areas of intraneural collagens were observed in the untreated (36.0 ± 5.8%, $p < 0.001$), MeCbl sheet (24.0 ± 8.3%, $p < 0.05$), and SIS sheet (33.7 ± 13.6%, $p < 0.001$) groups than in the sham group (8.5 ± 1.6%). Although there was no significant difference between the MeCbl and the SIS sheet group, the MeCbl sheet group showed a significantly lower collagen area than the untreated group ($p < 0.05$), whereas the SIS sheet group showed no difference compared with the untreated group (Fig. 4c).

Collagen infiltration is also thought to be caused by the invasion of inflammatory cells, fibroblasts, and other cells[48]. The number of DAPI + cells in the sciatic nerve harvested 2 weeks postoperatively was counted as a reflection of cell invasion (Fig. 5a). The untreated (1,678.2 ± 442.5/mm$^2$, $p < 0.001$), MeCbl sheet (1,186.1 ± 277.2/mm$^2$, $p < 0.001$), and SIS sheet (1,347.6 ± 161.7/mm$^2$, $p < 0.001$) groups had significantly higher number of DAPI + cells than the sham group (128.1 ± 44.2/mm$^2$), but only the MeCbl sheet group showed significantly lower values than the untreated group ($p < 0.05$) (Fig. 5b). Additionally, we counted the number of macrophages infiltrating the nerve to reflect initial inflammation and scar formation (Fig. 5a). The untreated (314.3 ± 75.8/mm$^2$, $p < 0.001$) and SIS sheet (290.4 ± 128.4/mm$^2$, $p < 0.001$) groups showed significantly higher number of macrophages than the sham group (22.4 ± 5.7/mm$^2$), whereas the MeCbl sheet group (87.1 ± 42.7/mm$^2$) showed no significant difference compared with the sham group. Moreover, it yielded significantly lower cell counts than both the untreated ($p < 0.001$) and SIS sheet groups ($p < 0.001$) (Fig. 5c). These results suggest that MeCbl sheets protect nerves from postoperative scarring and infiltration of inflammatory cells, fibroblasts, and other cells.

## Immunohistological evaluation of axon density and proportion of myelinated axons

Next, we examined whether MeCbl sheets alter the axon number and myelinated axon ratio, resulting from the protection of nerves from inflammatory cells and collagen infiltration. The number of axons, myelinated axon ratio, and distribution of each axonal diameter in the sciatic nerve were evaluated. The numbers of axons in the sham (12,805 ± 2958/mm$^2$, $p < 0.001$), MeCbl sheet (12,515 ± 2,527.6/mm$^2$, $p < 0.001$), and SIS sheet (11,372.8 ± 1,883.3/mm$^2$, $p < 0.001$) groups was significantly higher than that in the untreated group (5,584.7 ± 1,206.2/mm$^2$). There were no significant differences among the MeCbl sheet, SIS sheet, and sham groups (Fig. 6a, b). However, the myelinated axon ratio was significantly lower in the untreated (49.3 ± 7.1%, $p < 0.001$), MeCbl sheet (80.2 ± 4.3%, $p < 0.05$), and SIS sheet (71.1 ± 7.4%, $p < 0.001$) groups than in the sham group (92.1 ± 3.4%). However, the MeCbl sheet group showed a significantly higher myelinated axon ratio than the SIS sheet ($p < 0.05$) and untreated ($p < 0.001$) groups (Fig. 6c). Additionally, evaluation of the distribution of axons by diameter showed that the rate of thin axons < 2 μm in diameter was significantly higher in the SIS sheet group (41.2 ± 8.1%, $p < 0.05$) than in the MeCbl sheet group (27.6 ± 4%), whereas relatively thick axons between 4 and 6 μm in diameter were more common in the MeCbl sheet group (15.6 ± 3.6%, $p < 0.05$) than in the SIS sheet group (10.1 ± 1.3%). Furthermore, axons with diameters > 6 μm also tended to be more numerous in the MeCbl sheet group than in the SIS sheet group, although there were no significant differences between the

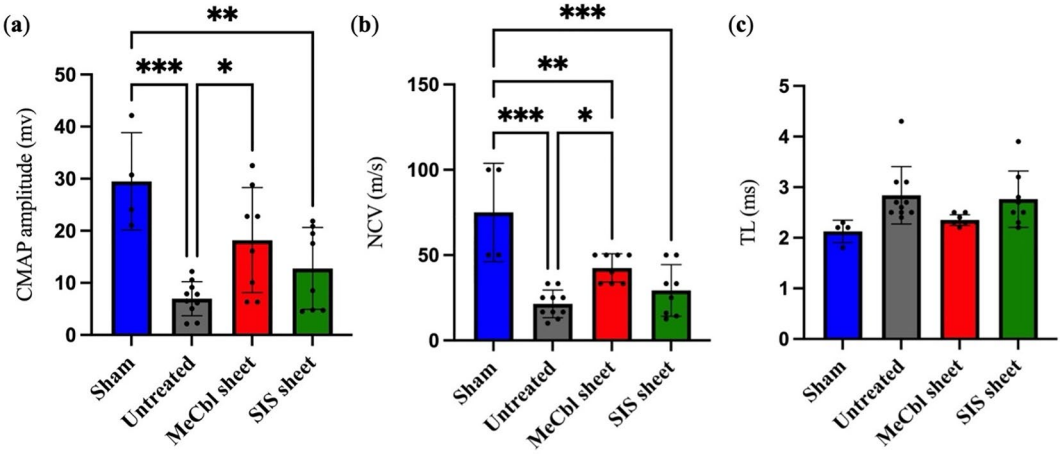


**Fig. 3**. Electrophysiological evaluation 2 weeks postoperatively. Methylcobalamin sheets mitigate the decrease in compound muscle action potential (CMAP) amplitude and nerve conduction velocity (NCV). (**a**) CMAP amplitude. (**b**) NCV. (**c**) Terminal latency. $^{*}p < 0.05$, $^{**}p < 0.01$, and $^{***}p < 0.001$, one-way analysis of variance followed by Tukey–Kramer's test.

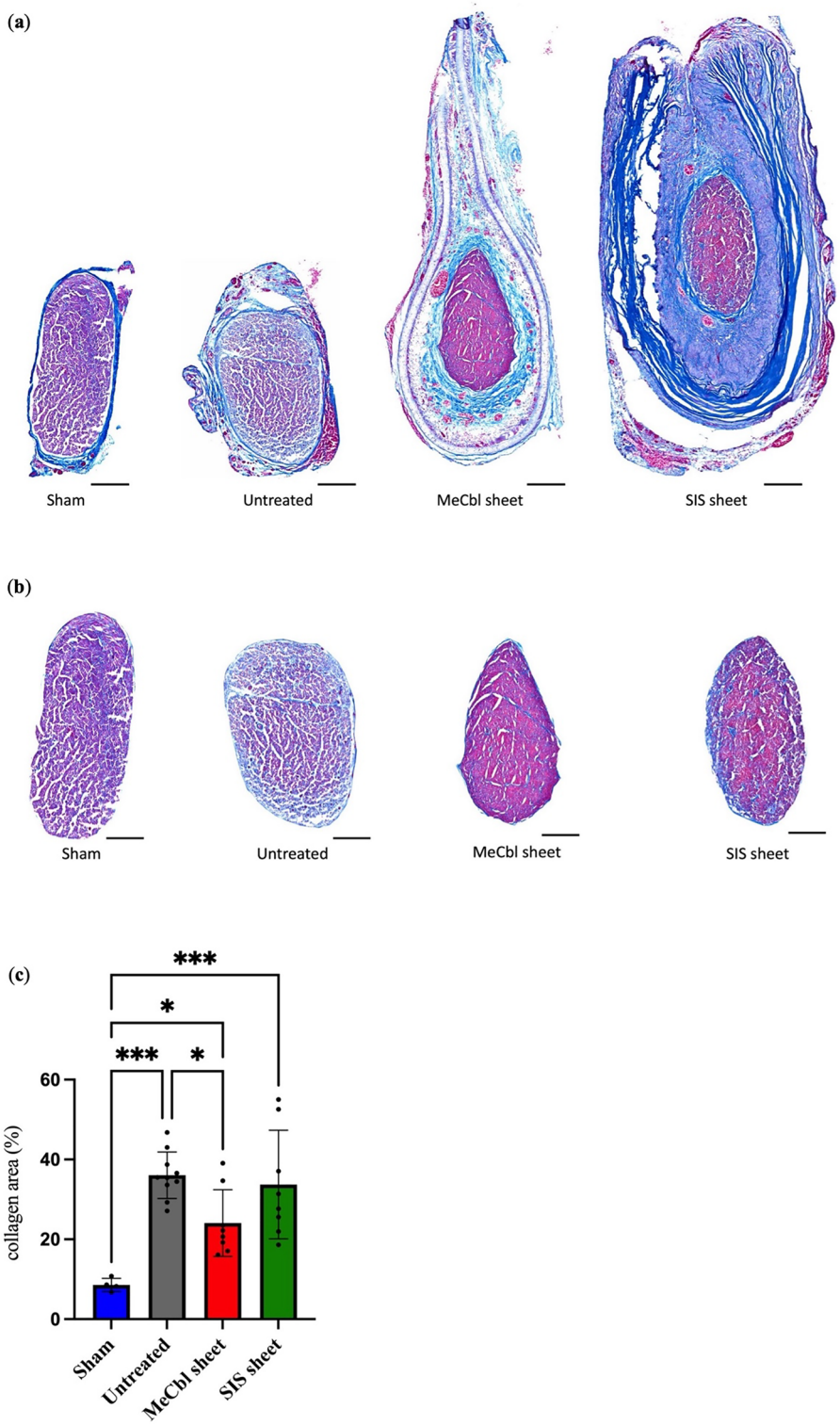


**Fig. 4**. Methylcobalamin sheets reduce intraneural collagen scar formation. (**a**) Representative cross-sectional slices of sciatic nerves with surrounding tissues stained with Masson's trichrome stain; scale bars = 200 µm. (**b**) Intraneural areas of sciatic nerves cropped using ImageJ stained with Masson's trichrome stain; scale bars = 200 µm. (**b**) Percentage of area of collagen infiltration into the nerve. $^{*}p < 0.05$, $^{***}p < 0.001$, one-way analysis of variance followed by Tukey–Kramer's test.

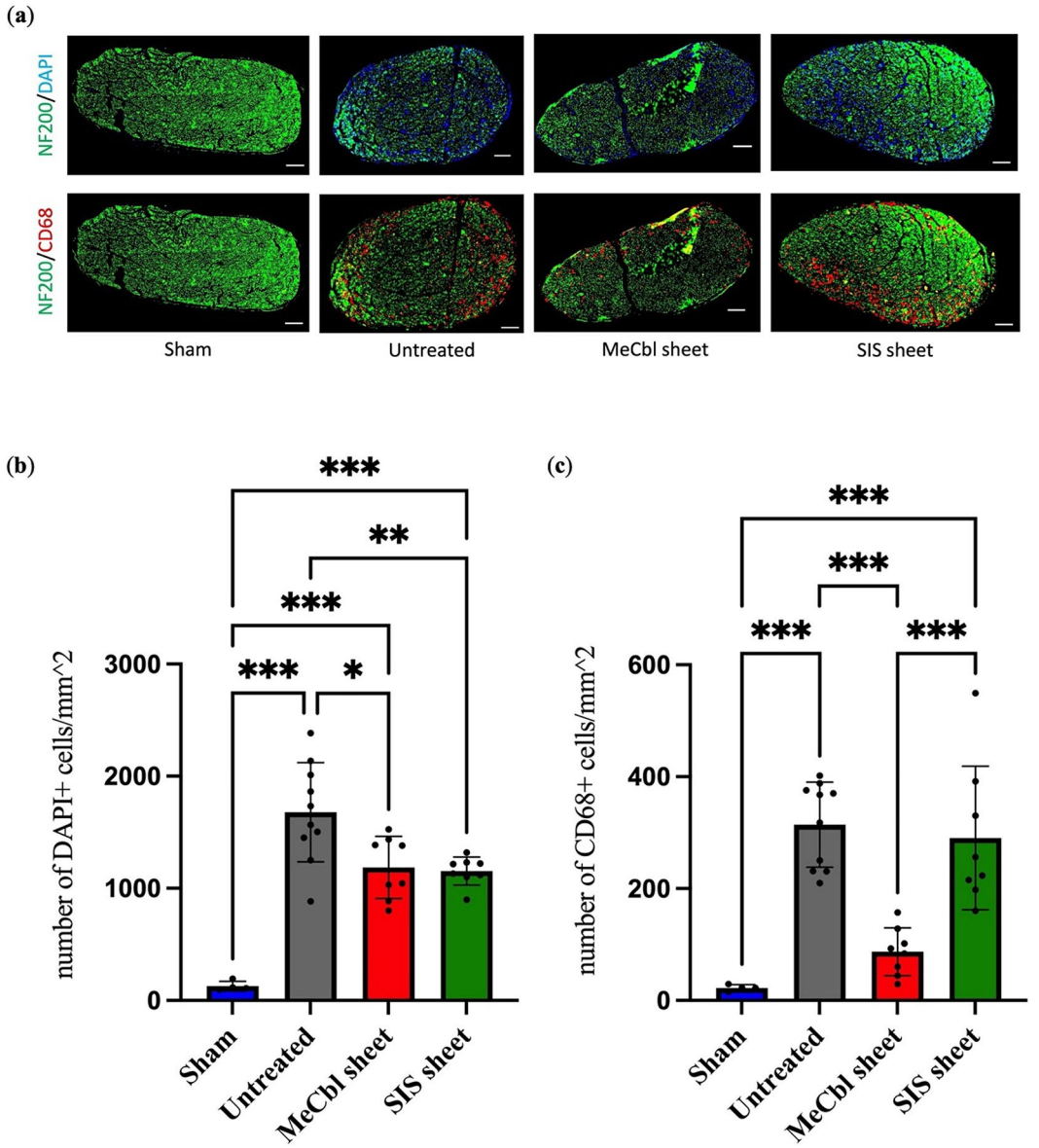


**Fig. 5**. Methylcobalamin sheets reduce intraneural cell and macrophage invasion. (**a**) Representative immunofluorescence micrographs showing cross-sectional slices of sciatic nerves labeled with 4',6-diamidino-2-phenylindole (DAPI) (blue) and CD68 (red) and neurofilament 200 (green) antibodies; scale bar = 100 μm. (**b**) The total numbers of intraneural DAPI + cells. (**c**) The total numbers of intraneural macrophages (CD68 + cells). $^{*}p < 0.05$, $^{**}p < 0.01$, and $^{***}p < 0.001$, one-way analysis of variance followed by Tukey–Kramer's test.

groups (Fig. 6d). These results suggest that MeCbl sheets prevent axonal degeneration and demyelination and the decline of motor and sensory functions and improve therapeutic outcomes.

## Discussion

In this study, the MeCbl sheet group exhibited significantly better results in terms of sensory and motor function tests and in electrophysiological examinations than the untreated group (Figs. 2 and 3). Additionally, there was significantly less infiltration of collagen and inflammatory cells within the nerve, and the MeCbl sheet group showed good results in terms of the residual axon count, axon diameter distribution, and myelination ratio compared with the untreated group (Figs. 4c and 5b and c, and 5d). Regarding the cause of nerve adhesions leading to nerve dysfunction, Masear and Colgin reported that demyelination and axonal degeneration were caused by compression, impaired gliding of the nerve, and inhibition of axonal extension due to infiltration of inflammatory cells and scar tissues into the nerve after peripheral nerve injury or decompression surgery [27]. This is consistent with the histological findings in this study, suggesting that the MeCbl sheet prevents inflammation and scar infiltration, thereby preventing demyelination and axonal degeneration.

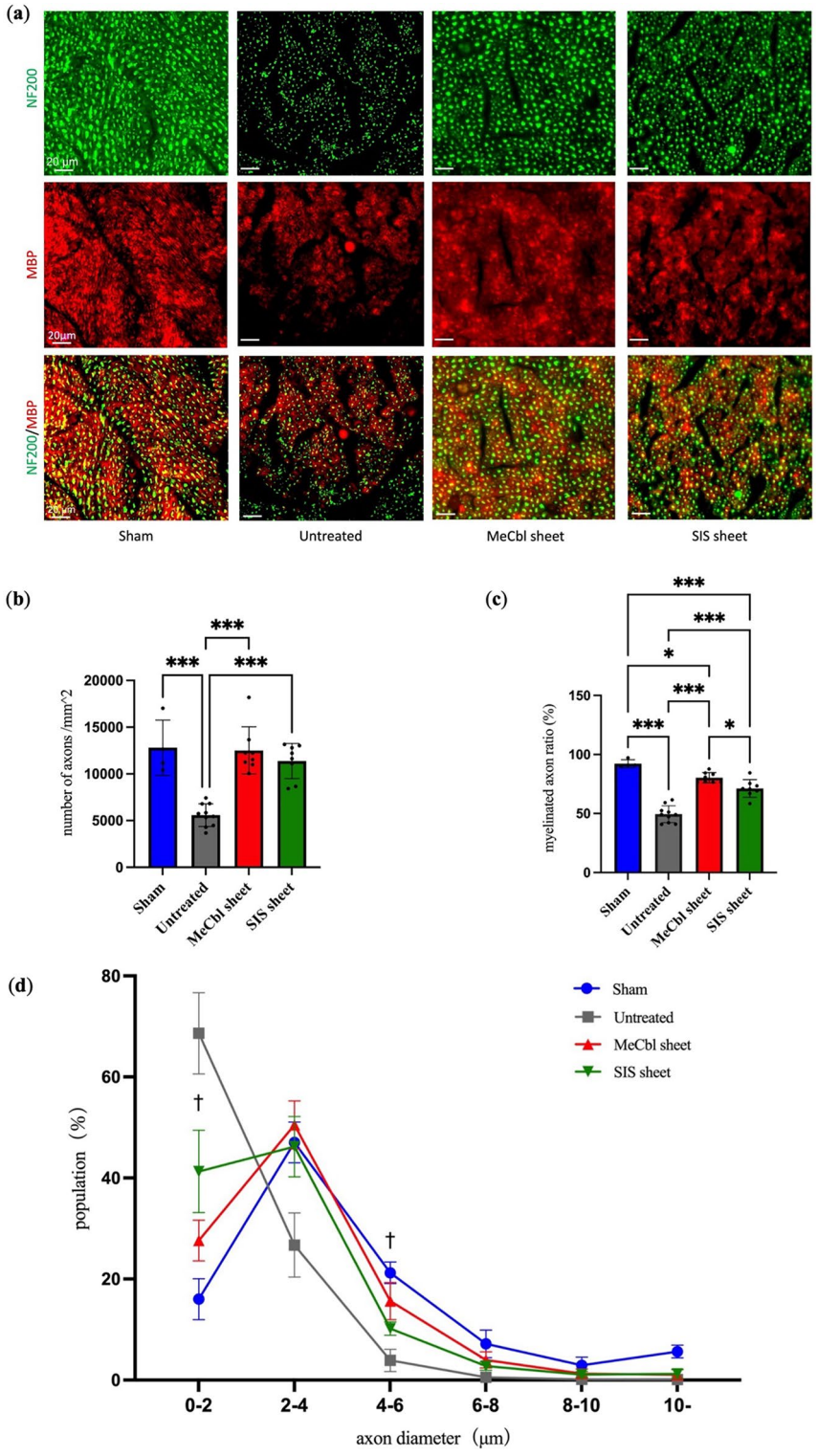


**Fig. 6**. Methylcobalamin (MeCbl) sheets mitigate the decrease of axons and proportion of myelinated axons and show larger axon diameter distribution. (**a**) Representative immunofluorescence micrographs showing cross-sectional slices of sciatic nerves with labeling for myelin basic protein (red) and neurofilament 200 (green); scale bars = 20 μm. (**b**) Total numbers of axons/mm$^2$. (**c**) Myelination ratio of total axons (%). (**d**) Population of axons according to diameter. Daggers (†) in the graph show only the relationship between the MeCbl and small intestinal submucosa sheet groups. $^{*}p < 0.05$, $^{**}p < 0.01$, and $^{***}p < 0.001$, $^{\dagger}p < 0.05$, one-way analysis of variance followed by Tukey–Kramer's test.

Another purpose of this study was to compare MeCbl sheets with sheets already in clinical use. SIS sheets, which were used as a comparison group in this study, improved the postoperative myelination ratio and number of axons in a rabbit sciatic nerve transection model and the results of electrophysiological examinations[20]. SIS sheets have also been used clinically, and their safety and efficacy in recurrent cases of carpal tunnel syndrome have already been reported [24]; their efficacy was similarly confirmed in our study (Figs. 2, 3, 4 and 5). Our results showed that MeCbl sheets were non-inferior to SIS sheets in several parameters or even significantly better in some parameters such as intraneural macrophage invasion, myelinated axon ratio, and axon diameter. This indicates that MeCbl sheets have better neuroprotective effects than SIS sheet and may be useful as new neuroprotective materials against inflammation and scar formation. Furthermore, vitamin B12 has an anti-inflammatory effect on nerve tissues[37,49–51]. Ehmedah et al. reported that vitamin B complex, including B12, attenuated neuroinflammatory responses by transforming macrophage polarization from proinflammatory (M1) to anti-inflammatory (M2) in a rat femoral nerve transection model[37]. Based on these results, the superiority of the MeCbl sheet group in this experiment is not only due to the barrier function of the MeCbl sheet, which suppressed cell infiltration, but also due to the anti-inflammatory and neuroregenerative effects of MeCbl. The combination of barrier function and anti-inflammatory and neuroregenerative effects of the sheet prevented adhesions to soft tissues outside the nerve and the infiltration of inflammatory cells into the nerve and the subsequent infiltration of fibroblasts and collagen fibers. This inhibited scar tissue formation, contributing to superior outcomes in terms of the residual axon count, axon diameter distribution, myelination ratio, sensory and motor function assessments, and electrophysiological evaluations when compared with those of the untreated and SIS sheet groups.

This study has the following limitations. First, a single-time endpoint of 2 weeks was used for all evaluations. Long-term outcomes, such as impaired sensory and motor functions, are unknown, and further studies using late endpoints after the scar proliferation period are necessary to gain further insights into the protective effects of MeCbl sheets. Second, we did not perform the SFI test. Although the SFI test is known to be a useful test for evaluating sciatic nerve function, we did not perform that in this study because the test is reported to be unreliable in the early stages of peripheral nerve injury[52]and, as previously reported[53], we found autotomy in our rat model, making it difficult to collect accurate data. Third, macrophage polarization was not evaluated. We found that the MeCbl sheet group had significantly fewer infiltrating macrophages within the nerve but did not reveal the ratio of M1 to M2 macrophages among the infiltrating macrophages in this study. However, based on the results obtained, it is assumed that the MeCbl sheets prevent macrophage infiltration, whereas the sustained release of MeCbl shifts the polarization of these macrophages from M1 to M2, thus suppressing inflammation. Fourth, there was no comparison with MeCbl-free PCL sheets in this study. Although the usefulness of PCL sheets has already been reported, no reports have compared them with MeCbl sheets. However, there are some reports that have compare PCL sheets and SIS sheets, and they reported that both PCL and SIS sheets showed neuroregenerative and anti-inflammatory effects, but there was no difference in macrophage infiltration into the nerve, which suggests inflammation, and no significant difference in the number of regenerative axons or axon diameter[25,30]. In this study, we found that the PCL sheet with methylcobalamin (MeCbl sheet) significantly inhibited macrophage infiltration into the nerve compared to the SIS sheet, and was superior in terms of the number of regenerating axons and axon diameter, unlike previous reports. Therefore, we hypothesized that MeCbl sheet is superior to the blank sheet, which is reported to have the same effect as the SIS sheet. Further studies are required to address these limitations.

In conclusion, to the best of our knowledge, this is the first study to investigate the neuroprotective effects of MeCbl sheets compared with those of other neuroprotective materials in a rat sciatic nerve adhesion model. The barrier function and anti-inflammatory effect of the MeCbl sheets alleviated postoperative inflammatory cell infiltration and scar formation and contributed to the maintenance of good nerve function, in contrast to the untreated group. This result was not inferior to that of the group using SIS sheets, and histological evaluation suggests that the neuroprotective function of MeCbl sheets may be superior to that of SIS sheets. Based on these results, we believe that MeCbl sheets may be useful as a new material to prevent nerve injury caused by post-inflammatory adhesions.

## Data availability

All data analyzed in this study are available from the corresponding author upon request.

Received: 12 January 2024; Accepted: 5 November 2024
Published online: 06 January 2025

## References

1. Kadzielski, J. et al. Evaluation of preoperative expectations and patient satisfaction after carpal tunnel release. *J. Hand Surg. Am.* **33**, 1783–1788. https://doi.org/10.1016/j.jhsa.2008.06.019 (2008).
2. Li, Y. et al. Open versus endoscopic carpal tunnel release: a systematic review and meta-analysis of randomized controlled trials. *BMC Musculoskelet. Disord.* **21**, 272. https://doi.org/10.1186/s12891-020-03306-1 (2020).
3. Wojewnik, B. & Bindra, R. Cubital tunnel syndrome - review of current literature on causes, diagnosis and treatment. *J. Hand Microsurg.* **1**, 76–81. https://doi.org/10.1007/s12593-009-0020-9 (2009).
4. Graf, A., Ahmed, A. S., Roundy, R., Gottschalk, M. B. & Dempsey, A. Modern Treatment of Cubital tunnel syndrome: evidence and controversy. *J. Hand Surg. Glob Online.* **5**, 547–560. https://doi.org/10.1016/j.jhsg.2022.07.008 (2023).
5. Abe, Y., Doi, K. & Kawai, S. An experimental model of peripheral nerve adhesion in rabbits. *Br. J. Plast. Surg.* **58**, 533–540. https://doi.org/10.1016/j.bjps.2004.05.012 (2005).
6. Lundborg, G. & Rydevik, B. Effects of stretching the tibial nerve of the rabbit. A preliminary study of the intraneural circulation and the barrier function of the perineurium. *J. Bone Joint Surg. Br.* **55**, 390–401 (1973).

7. McCall, T. D., Grant, G. A., Britz, G. W., Goodkin, R. & Kliot, M. Treatment of recurrent peripheral nerve entrapment problems: role of scar formation and its possible treatment. *Neurosurg. Clin. N Am.* **12**, 329–339 (2001).
8. Millesi, H., Zoch, G. & Rath, T. The gliding apparatus of peripheral nerve and its clinical significance. *Ann. Chir. Main Memb. Super.* **9**, 87–97. https://doi.org/10.1016/s0753-9053(05)80485-5 (1990).
9. Koh, T. J. & DiPietro, L. A. Inflammation and wound healing: the role of the macrophage. *Expert Rev. Mol. Med.* **13**, e23. https://doi.org/10.1017/S1462399411001943 (2011).
10. Martin, P. Wound healing–aiming for perfect skin regeneration. *Science.* **276**, 75–81. https://doi.org/10.1126/science.276.5309.75 (1997).
11. Pull, S. L., Doherty, J. M., Mills, J. C., Gordon, J. I. & Stappenbeck, T. S. Activated macrophages are an adaptive element of the colonic epithelial progenitor niche necessary for regenerative responses to injury. *Proc. Natl. Acad. Sci. U S A.* **102**, 99–104. https://doi.org/10.1073/pnas.0405979102 (2005).
12. Steed, D. L. The role of growth factors in wound healing. *Surg. Clin. North. Am.* **77**, 575–586. https://doi.org/10.1016/s0039-6109(05)70569-7 (1997).
13. Nagaraja, S. et al. Predictive Analysis of Mechanistic Triggers and Mitigation Strategies for pathological scarring in skin wounds. *J. Immunol.* **198**, 832–841. https://doi.org/10.4049/jimmunol.1601273 (2017).
14. Dahlin, L. B., Lekholm, C., Kardum, P. & Holmberg, J. Coverage of the median nerve with free and pedicled flaps for the treatment of recurrent severe carpal tunnel syndrome. *Scand. J. Plast. Reconstr. Surg. Hand Surg.* **36**, 172–176. https://doi.org/10.1080/02844310275371806 9 (2002).
15. Fusetti, C., Garavaglia, G., Mathoulin, C., Petri, J. G. & Lucchina, S. A reliable and simple solution for recalcitrant carpal tunnel syndrome: the hypothenar fat pad flap. *Am. J. Orthop. (Belle Mead NJ).* **38**, 181–186 (2009).
16. Uemura, T., Takamatsu, K., Okada, M., Ikeda, M. & Nakamura, H. Radial artery perforator adiposal flap for coverage of the scarred median nerve. *J. Plast. Reconstr. Aesthet. Surg.* **66**, 1019–1021. https://doi.org/10.1016/j.bjps.2013.01.024 (2013).
17. Braga-Silva, J. The use of silicone tubing in the late repair of the median and ulnar nerves in the forearm. *J. Hand Surg. Br.* **24**, 703–706. https://doi.org/10.1054/jhsb.1999.0276 (1999).
18. Dahlin, L. & Lundborg, G. The use of silicone tubing in the late repair of the median and ulnar nerves in the forearm. *J. Hand Surg. Br.* **26**, 393–394. https://doi.org/10.1054/jhsb.2001.0561 (2001).
19. Garrett, R., Niiyama, E., Kotsuchibashi, Y., Uto, K. & Ebara, M. Biodegradable nanofiber for delivery of Immunomodulating Agent in the treatment of basal cell carcinoma. *Fibers.* **3**, 478–490. https://doi.org/10.3390/fib3040478 (2015).
20. Kokkalis, Z. T. et al. Assessment of processed porcine extracellular matrix as a protective barrier in a rabbit nerve wrap model. *J. Reconstr. Microsurg.* **27**, 19–28. https://doi.org/10.1055/s-0030-1267379 (2011).
21. Lee, S. Y., Thow, S. Y., Abdullah, S. & Ng, M. H. Mohamed Haflah, N. H. Advancement of Electrospun Nerve Conduit for peripheral nerve regeneration: a systematic review (2016–2021). *Int. J. Nanomed.* **17**, 6723–6758. https://doi.org/10.2147/IJN.S362144 (2022).
22. Lopez, J. et al. Poly(epsilon-Caprolactone) Nanofiber Wrap improves nerve regeneration and functional outcomes after delayed nerve repair. *Plast. Reconstr. Surg.* **144**, 48e–57e. https://doi.org/10.1097/PRS.0000000000005715 (2019).
23. Meek, M. F., Coert, J. H., Hermens, R. A. & Nicolai, J. P. The use of silicone tubing in the late repair of the median and ulnar nerves in the forearm. *J. Hand Surg. Br.* **25**, 408–409. https://doi.org/10.1054/jhsb.2000.0438 (2000).
24. Power, D., Jordaan, P. & Uhiara, O. Management of the scarred nerve using porcine submucosa extracellular matrix nerve wraps. *J. Musculoskelet. Surg. Res.* **3** https://doi.org/10.4103/jmsr.jmsr_69_18 (2019).
25. Sarhane, K. A. et al. Macroporous nanofiber wraps promote axonal regeneration and functional recovery in nerve repair by limiting fibrosis. *Acta Biomater.* **88**, 332–345. https://doi.org/10.1016/j.actbio.2019.02.034 (2019).
26. Tos, P. et al. Efficacy of anti-adhesion gel of carboxymethylcellulose with polyethylene oxide on peripheral nerve: experimental results on a mouse model. *Muscle Nerve.* **53**, 304–309. https://doi.org/10.1002/mus.24739 (2016).
27. Masear, V. R. & Colgin, S. The treatment of epineural scarring with allograft vein wrapping. *Hand Clin.* **12**, 773–779 (1996).
28. Murakami, K. et al. Vein wrapping for chronic nerve constriction injury in a rat model: study showing increases in VEGF and HGF production and prevention of pain-associated behaviors and nerve damage. *J. Bone Joint Surg. Am.* **96**, 859–867. https://doi.org/10.2106/JBJS.L.01790 (2014).
29. Shintani, K. et al. Protective effect of biodegradable nerve conduit against peripheral nerve adhesion after neurolysis. *J. Neurosurg.* **129**, 815–824. https://doi.org/10.3171/2017.4.JNS162522 (2018).
30. Shim, S. W. et al. Evaluation of small intestine submucosa and poly(caprolactone-co-lactide) conduits for peripheral nerve regeneration. *Tissue Eng. Part. A.* **21**, 1142–1151. https://doi.org/10.1089/ten.TEA.2014.0165 (2015).
31. Li, Q., Li, T., Cao, X. C., Luo, D. Q. & Lian, K. J. Methylprednisolone microsphere sustained-release membrane inhibits scar formation at the site of peripheral nerve lesion. *Neural Regen Res.* **11**, 835–841. https://doi.org/10.4103/1673-5374.182713 (2016).
32. Li, Y. et al. Minocycline alleviates peripheral nerve adhesion by promoting regulatory macrophage polarization via the TAK1 and its downstream pathway. *Life Sci.* **276**, 119422. https://doi.org/10.1016/j.lfs.2021.119422 (2021).
33. Sato, Y., Honda, Y., Iwamoto, J., Kanoko, T. & Satoh, K. Amelioration by mecobalamin of subclinical carpal tunnel syndrome involving unaffected limbs in stroke patients. *J. Neurol. Sci.* **231**, 13–18. https://doi.org/10.1016/j.jns.2004.12.005 (2005).
34. Okada, K. et al. Methylcobalamin increases Erk1/2 and akt activities through the methylation cycle and promotes nerve regeneration in a rat sciatic nerve injury model. *Exp. Neurol.* **222**, 191–203. https://doi.org/10.1016/j.expneurol.2009.12.017 (2010).
35. Nishimoto, S. et al. Methylcobalamin promotes the differentiation of Schwann cells and remyelination in lysophosphatidylcholine-induced demyelination of the rat sciatic nerve. *Front. Cell. Neurosci.* **9**, 298. https://doi.org/10.3389/fncel.2015.00298 (2015).
36. Okada, K. et al. Akt/mammalian target of rapamycin signaling pathway regulates neurite outgrowth in cerebellar granule neurons stimulated by methylcobalamin. *Neurosci. Lett.* **495**, 201–204. https://doi.org/10.1016/j.neulet.2011.03.065 (2011).
37. Ehmedah, A. et al. Vitamin B complex treatment attenuates local inflammation after peripheral nerve Injury. *Molecules.* **24** https://doi.org/10.3390/molecules24244615 (2019).
38. Suzuki, K. et al. Electrospun nanofiber sheets incorporating methylcobalamin promote nerve regeneration and functional recovery in a rat sciatic nerve crush injury model. *Acta Biomater.* **53**, 250–259. https://doi.org/10.1016/j.actbio.2017.02.004 (2017).
39. Nava-Ocampo, A. A., Pastrak, A., Cruz, T. & Koren, G. Pharmacokinetics of high doses of cyanocobalamin administered by intravenous injection for 26 weeks in rats. *Clin. Exp. Pharmacol. Physiol.* **32**, 13–18. https://doi.org/10.1111/j.1440-1681.2005.04145.x (2005).
40. Miyamura, S. et al. A nanofiber sheet incorporating vitamin B12 promotes nerve regeneration in a rat Neurorrhaphy Model. *Plast. Reconstr. Surg. Glob Open.* **7**, e2538. https://doi.org/10.1097/GOX.0000000000002538 (2019).
41. Sayanagi, J. et al. Combination of Electrospun Nanofiber Sheet Incorporating Methylcobalamin and PGA-Collagen Tube for treatment of a sciatic nerve defect in a rat model. *J. Bone Joint Surg. Am.* **102**, 245–253. https://doi.org/10.2106/JBJS.19.00254 (2020).
42. Graham, M., Pitcher, J. R. & Henry, J. L. Paw withdrawal threshold in the Von Frey hair test is influenced by the surface on which the rat stands. *J. Neurosci. Methods.* **87**, 185–193 (1999).
43. Navarro, X. Functional evaluation of peripheral nerve regeneration and target reinnervation in animal models: a critical overview. *Eur. J. Neurosci.* **43**, 271–286. https://doi.org/10.1111/ejn.13033 (2016).
44. Cheah, M., Fawcett, J. W. & Andrews, M. R. Assessment of Thermal Pain sensation in rats and mice using the Hargreaves Test. *Bio Protoc.* **7** https://doi.org/10.21769/BioProtoc.2506 (2017).
45. Hargreaves, K., Dubner, R., Brown, F., Flores, C. & Joris, J. A new and sensitive method for measuring thermal nociception in cutaneous hyperalgesia. *Pain.* **32**, 77–88. https://doi.org/10.1016/0304-3959(88)90026-7 (1988).

46. Shin, R. H. et al. Isometric tetanic force measurement method of the tibialis anterior in the rat. *Microsurgery*. **28**, 452–457. https://doi.org/10.1002/micr.20520 (2008).
47. Kanda, Y. Investigation of the freely available easy-to-use software 'EZR' for medical statistics. *Bone Marrow Transpl.* **48**, 452–458. https://doi.org/10.1038/bmt.2012.244 (2013).
48. Gabbiani, G. & Majne, R. G. Presence of modified fibroblasts in granulation tissue and their possible role in wound contraction. *Experientia*. **15**, 549–550 (1971).
49. Nemazannikova, N., Mikkelsen, K., Stojanovska, L., Blatch, G. L. & Apostolopoulos, V. Is there a link between vitamin B and multiple sclerosis? *Med. Chem.* **14**, 170–180. https://doi.org/10.2174/1573406413666170906123857 (2018).
50. Arora, K. et al. Neuropathology of vitamin B(12) deficiency in the Cd320(-/-) mouse. *FASEB J.* **33**, 2563–2573. https://doi.org/10.1096/fj.201800754RR (2019).
51. Nuru, M., Muradashvili, N., Kalani, A., Lominadze, D. & Tyagi, N. High methionine, low folate and low vitamin B6/B12 (HM-LF-LV) diet causes neurodegeneration and subsequent short-term memory loss. *Metab. Brain Dis.* **33**, 1923–1934. https://doi.org/10.1007/s11011-018-0298-z (2018).
52. Monte-Raso, V. V., Barbieri, C. H., Mazzer, N., Yamasita, A. C. & Barbieri, G. Is the sciatic functional index always reliable and reproducible? *J. Neurosci. Methods*. **170**, 255–261. https://doi.org/10.1016/j.jneumeth.2008.01.022 (2008).
53. Medeiros, P. et al. An adapted chronic Constriction Injury of the sciatic nerve produces sensory, affective, and cognitive impairments: a Peripheral Mononeuropathy Model for the study of Comorbid Neuropsychiatric Disorders Associated with Neuropathic Pain in rats. *Pain Med.* **22**, 338–351. https://doi.org/10.1093/pm/pnaa206 (2021).


## Acknowledgements

This study was supported by Nippon Zoki Pharmaceutical Co., Ltd., Japan. We thank all the members of Okada's laboratory for their helpful discussions and comments. The authors would like to thank Editage (www.editage.jp) for the English language review.

## Author contributions

Y.Y., T.I., and H.T. performed most of the experiments. Y.Y., T.I., T.K., T.S., K.K., A.K., and H.T. conceptualized the study and wrote the manuscript. T.I., M.K., A.K., R.S., S.M., K.O., S.O., and H.T. supported and helped write the manuscript. All the authors have read and approved the final submission of this paper.

## Declarations

## Competing interests

The authors declare no competing interests.

## Additional information

**Correspondence** and requests for materials should be addressed to H.T.

**Reprints and permissions information** is available at www.nature.com/reprints.

**Publisher's note** Springer Nature remains neutral with regard to jurisdictional claims in published maps and institutional affiliations.